Frontal Process Zone Toughening Mechanism of Ceramic-Based Nanocomposites

H. Awaji and S-M. Choi

Nagoya Institute of Technology, Gokiso-cho, Showa-ku, Nagoya 466-8555, Japan

ABSTRACT: *Toughening mechanism for ceramic-based nanocomposites will be presented based on residual stresses around second-phase nano-particles dispersed in matrix grains. The residual thermal stresses around a spherical particle within a concentric sphere of a matrix grain were analyzed to clarify the effects of residual stresses on the toughening mechanism in the frontal process zone. An indirect estimation technique for assessing a critical size of the frontal process zone in ceramics was also proposed using a SEVNB (Single-Edge V-Notched Beam) technique. A three-point flexure test was carried out for nanocomposites and monolithic materials with various depths of a sharp V-shaped notch, and then a critical local stress was calculated at a distance from the notch tip. The frontal process zone size at the beginning of crack propagation, namely, the critical frontal process zone size, was determined as the distance from the notch tip to the point where the local stress has the same value as the flexural strength of the material. The results revealed that both the strength and the critical frontal process zone size must be increased for enhancement of the fracture toughness of ceramics.*

INTRODUCTION

In the past several decades, much effort has been concentrated on improving the fracture toughness of ceramics and many techniques have been proposed. The toughening techniques can be classified into three groups: (A) particle-dispersion toughening, (B) multi-layered toughening, and (C) phase-transformation toughening. For the technique (A), several kinds of particles are used, such as whiskers, platelets, ductile particles, and so on. Newly developed nanocomposites proposed by Niihara [1] are also included in this group. However, the nanocomposites have different mechanisms of toughening and strengthening among them. The microstructure of the nanocomposites is formed by nano-size second-phase particles dispersed within the matrix grains and/or on the grain boundaries, and indicates a marked improvement of strength and a moderate enhancement of toughness [1]. Also, Davidge, et al. [2] conducted a multinational project and confirmed improvements of mechanical properties in nanocomposites.

In this paper, we focus our attention on the frontal process zone toughening mechanism of nanocomposites and propose a novel technique for estimating a critical size of a frontal process zone in ceramics, using a single-edge V-notched beam (SEVNB) technique [3,4]. Based on a local fracture criterion under linear fracture mechanics, critical local stress is calculated at a certain critical distance from the notch tip. The critical size of the frontal process zone is determined as the distance between the notch tip and the point where the critical local stress has the same value as the flexure strength of the material [5].

RESULTS AND DISCUSSION

Residual Stresses Around a Particle

To examine effects of residual stresses around particles on toughening mechanism in nanocomposites, we consider a simple model consisting of a spherical particle within a concentric matrix sphere, as shown in Fig. 1. Due to limitations of space, the explanation of the analytical technique will be omitted here [6].

Figure 2 compares the stresses in the matrices of infinite and finite spheres. It is noted that the stresses in the finite sphere are greater than those in the infinite sphere and that the stresses reduce to zero with distance from the particle/matrix boundary, except that the hoop stress in the finite sphere has a finite value on its spherical edge. These stress distributions indicate that lattice defects will be created only in close vicinity to the particle/matrix boundaries especially around a nano-size particle, which generates the toughening and strengthening mechanisms in nanocomposites [6].

Table 1 shows the residual stresses along the particle/matrix boundary in nanocomposite systems fabricated by Niihara [1], where a/b = 1/5 and θ_0 =

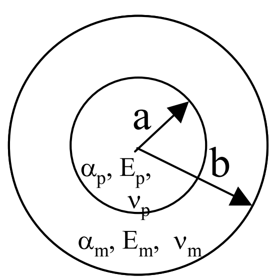

Figure 1: A spherical particle within a concentric sphere of matrix grain.

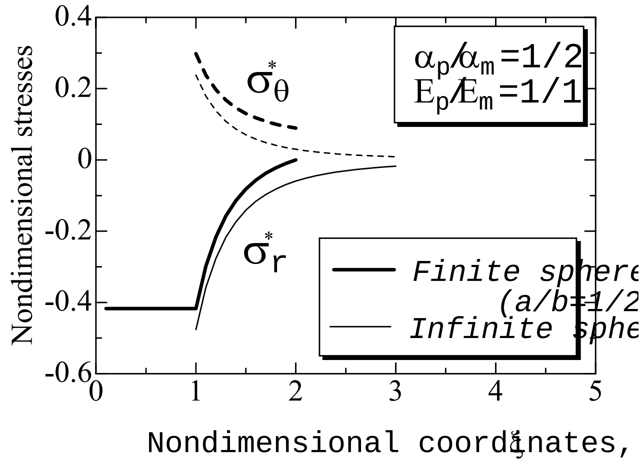

Figure 2: Stresses in matrices of infinite and finite spheres.

TABLE 1: Residual stresses along a particle/matrix boundary in nanocomposites.

Systems	α_m/α_p $\times 10^{-6}$ K^{-1}	E_m/E_p GPa	ν_m/ν_p	Stresses on the boundary	
				σ_θ GPa	τ_{max} GPa
Al_2O_3/SiC	8.8/4.7	380/490	0.21/0.19	1.1.6	1.71
Si_3N_4/SiC	2.6/4.7	280/490	0.26/0.19	-0.48	0.70

1,570ºC were assumed. It is noted that there are large maximum shear stresses on the boundary especially in the alumina/silicon carbide system, and that these stresses are large enough to create lattice defects around the particle.

Toughening Mechanism in Nanocomposites

From the analytical results mentioned above, we recognize that the mismatch in thermal expansion between the matrix and dispersed nano-size particles mainly generates large residual stresses around the particles. However, these stresses reduce quickly with the distance from the boundary because of the small size of particles, which can yield lattice defects in close vicinity to the particles during the cooling process. Further annealing of nanocomposites will lead to the development of sub-grain boundaries or dislocation networks around the particles. This microstructure will create many nanocracks along the sub-grain boundaries when a main crack approaches, and the nanocracks can be expected to expand the size of the frontal process zone, which

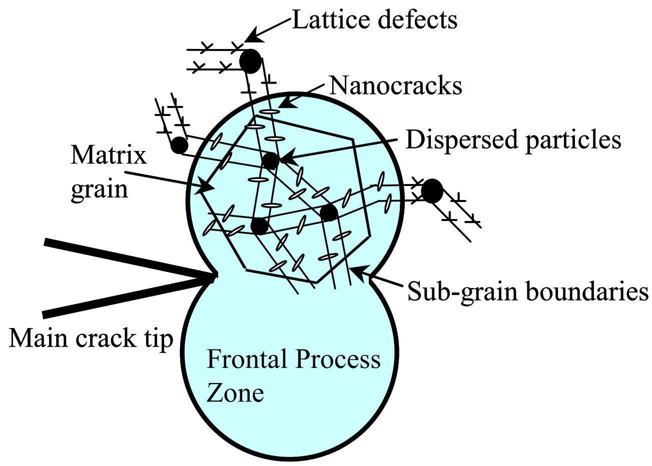

Figure 3: Schematic of a toughening mechanism in nanocomposites.

improves the fracture toughness of the material. The toughening mechanism in nanocomposites is therefore considered to be expansion mechanism of the frontal process zone size [7,8]. The schematic explanation of the frontal process zone toughening mechanism is shown in Figure 3. Because dislocations have difficulty moving in ceramics, the lattice defects, such as dislocations, can operate as nanocrack nuclei in highly stressed areas. The important point for enhancing the toughness of ceramic-based nanocomposites is, therefore, to create dispersed lattice defects in the matrix. If cracks instead of lattice defects are created around the second-phase particles, the cracks cannot move within a matrix grain and do not expand the frontal process zone size. Therefore, controlling the temperature-time schedule during sintering or annealing is requisite to fabricate nanocomposites with improved fracture toughness.

A technique for estimating the critical frontal process zone size, which will be discussed later, revealed that the critical size of monolithic alumina was about 11μm [5]. The fact indicates that the effective nanocracks to expand the FPZ size must be smaller than roughly 1μm in alumina.

Estimation of Critical Frontal Process Zone Size

A novel technique is proposed to estimate the critical size of the frontal process zone in ceramics using a SEVNB technique [3,4]. Based on a local fracture criterion under linear fracture mechanics, critical local stress, σ_c, is calculated at a critical distance from the notch tip, r_0. Therefore, the relationship among the fracture toughness, K_{IC}, σ_c, and r_0 is expressed as

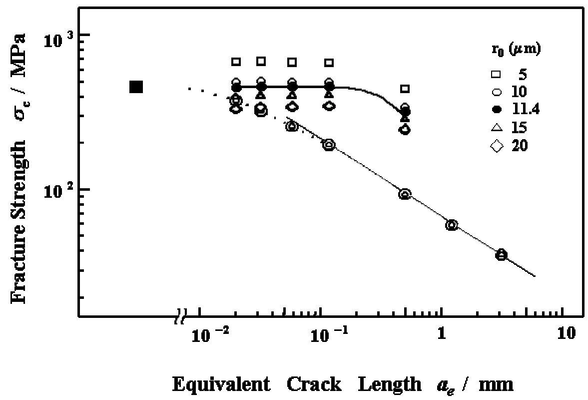

Figure 4: Relationship between the fracture strength and equivalent crack length of alumina.

long as the condition of small scale yielding is satisfied as

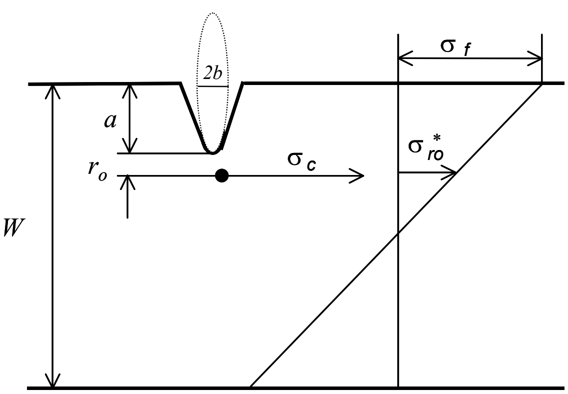

Figure 5: Specimen shape and remote stresses.

$$\sigma_C = \frac{K_{IC}}{\sqrt{2\pi r_0}} \tag{1}$$

Flexural specimens of 3×4×40 mm^3 in size with various V-notch depths were used for measuring the strength. The material used was polycrystalline alumina of 99.5 % purity with a minor additive of MgO, manufactured by Japan Fine Ceramics Center, and the mean grain size of 4 μm with isotropic morphology and homogeneous microstructure.

The experimental results are shown in Figure 4, where the horizontal axis indicates an equivalent crack length, a_e, calculated as

$$a_e = \frac{Y^2}{\pi} a \qquad (2)$$

where Y represents the shape factor of the notched specimen and *a* the length of the edge notch. In Figure 4, the marks (◎) indicate the strength of the specimen with various depths of a V-notch, and the mark (■) is the strength of the specimen with smooth surfaces.

A technique for estimating the critical frontal process zone size is expressed as follows: The remote flexural stress at the critical point from the notch tip, σ_{r0}^*, is simply assumed for a shallow notch as

$$\sigma_{r_0}^* \approx \sigma_f \frac{W/2-(a+r_0)}{W/2} \qquad (3)$$

where σ_f represents flexural strength of the material and W the height of the specimen, shown in Figure 5. Then, the critical local stress, σ_C, at r_0 is calculated as

$$\begin{aligned} &\sigma_C = \sigma_{r_0}^* F(r_0) \\ &F(r_0) = \frac{1}{2}\left\{1+\frac{2(1+m)}{\alpha^2-m}\right\} + \frac{1}{2}\left[1+\frac{m^2-1}{\alpha^2-m}\left\{1+\frac{m-1}{\alpha^2-m}\frac{3\alpha^2-m}{\alpha^2-m}\right\}\right] \end{aligned} \qquad (4)$$

where *m* is $(a-b)/(a+b)$, *a* and *b* are the semi major and semi minor axes of the elliptical hole, respectively, and $F(r_0)$ the non-dimensional stress distribution at the distance r_0 from the notch tip. $F(r_0)$ is derived from the exact solution of stress distribution along the major axis of an elliptical hole analyzed by Williams [9].

The critical local stresses calculated at several distances r_0 for alumina are shown in Figure 4 using five different marks (□, ○, ●, Δ, and ◊). The critical local stresses in the figure lie on the horizontal lines except for the longest crack length, where the approximation of σ_{r0}^* defined in Eq. 3 is not appropriate in this case.

It is evident that the critical local stress of r_0 = 11.4 μ*m* in Figure 4 is in good agreement with the flexural strength of the specimen with no artificial notch. Therefore, the value of 11.4 μ*m* is estimated to be the critical frontal process zone size of alumina.

Figure 6 shows the relationship between the fracture toughness and the product of critical stress and square root of the critical frontal process zone size for several materials, such as alumina mentioned previously, silicon nitride (Refer-ceram SN, Japan Fine Ceramics Center), isotropic graphite

TABLE 2: Summary of experimental data.

Materials	K_{IC} /MPa m$^{1/2}$	σ_c /MPa	r_0 /μm
Si_3N_4	6.70	1105	4.9
Al_2O_3	3.72	462	11
ISO-88	1.24	120	14

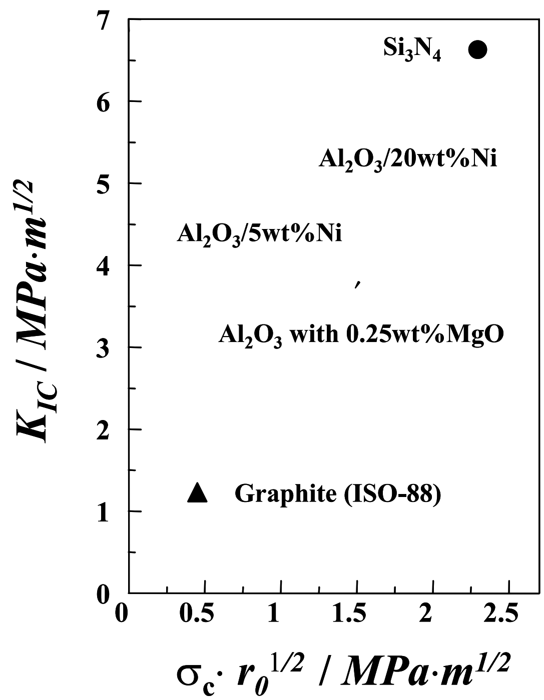

Figure 6: Relationship between K_{IC} and $\sigma_c r_0^{1/2}$

(ISO-88, TOYO Tanso, Japan), and alumina/nickel nanocomposites fabricated by Choi, et al. [10]. It is recognized that there is almost linear relationship between K_{IC} and $\sigma_c \cdot r_0^{1/2}$.

Table 2 shows the experimental data of these materials. It is noted that the smallest critical distance among them is 4.79 μm for Si_3N_4. However, the strength of Si_3N_4 is the highest, and subsequently, the fracture toughness is the highest. On the contrary, the largest critical distance is 12.5 μm for ISO-88, but the material exhibits low strength, and the fracture toughness is also low. This fact suggests that both the strength and critical distance must be increased for enhancing fracture toughness of ceramics.

CONCLUSIONS

Frontal process zone toughening mechanism in particle-dispersed composites, especially nanocomposites, is examined based on the analytical results of residual stresses around the dispersed particles. Critical sizes of frontal process zone in several materials including alumina/nickel nanocomposites are estimated using the V-shaped notch technique, based on the local fracture criterion. The critical frontal process zone size was determined to be the distance at which the critical local stress has the same value as the flexure strength of the material. The relationship among the critical frontal process zone size, the fracture toughness, and the flexure strength was discussed. The results revealed that the strength and the critical frontal process zone size must be increased for enhancing the fracture toughness of ceramics.

REFERENCES

1. Niihara, K (1991) *J. Ceram. Soc. Japan* **99**, 974.
2. Davidge, R.W., Brook, R.J., Cambier, F., Poorteman, M., Leriche, A., O'Sullivan, D., Hampshire, S., and Kennedy, T. (1997) *British Ceram. Trans.* **96**, 121.
3. Awaji, H. and Sakaida, Y. (1990) *J. Am. Ceram. Soc.* **73**, 3522.
4. Awaji, H., Watanabe, T., Sakaida, Y., and Nakagawa H. (1992) *Ceramics Int.* **18**, 11.
5. Awaji, H., Choi, S-M., and Jayaseelan, D. D. (2001) *J. Ceram. Soc. Japan* **109**, 591.
6. Choi, S-M., Yagi, E., Nishikawa, T. and Awaji, H., (2001) *J. Soc. Mater. Sci., Japan* (submitted).
7. Hoagland, R.G. and Embury, J.D. (1980) *J. Am. Ceram. Soc.* **63**, 404.
8. Evans, A.G. and Faber, K.T. (1984) *J. Am. Ceram. Soc.* **67**, 255.
9. Williams, J. G. (1973) *Stress Analysis of polymers*, Longman, London.
10. Choi, S-M., Okamoto, M., and Awaji, H., *Proceedings of IGTI 2002*, GT-2002-30508, June 3-6, Amsterdam.